STEADY-STATE MODELLING OF FALLING FILM DRAIN WATER HEAT RECOVERY PERFORMANCE USING RATED DATA

R. Manouchehri, M. Collins
University of Waterloo, Department of Mechanical and Mechatronics Engineering
Waterloo, Ontario, Canada

ABSTRACT

Drain water heat recovery (DWHR) systems recover heat from a building's greywater and use it to preheat incoming mains water. The rated effectiveness of such systems is typically determined at a fixed temperature difference and flow rate, and under steady-state and equal flow conditions. Unfortunately, this may not be representative of what is actually occurring during operation. The present work attempts to bridge this gap by producing correlations that are capable of predicting steady-state performance based on data produced during the rating process.

DWHR system performance turns out to be highly predictable, regardless of system size or coil design. Starting with rated data, one can reliably find the performance as a function of flow rate, adjust the results for different inlet water temperatures, and then account for non-equal flow conditions. Experiments show that the complete model is able to predict heat transfer rates to within about 2.5%.

INTRODUCTION

It is well understood that global energy consumption is steadily increasing, and that energy conservation will play a key role in allowing utilities to meet future energy demands. The energy used to heat water for domestic purposes is no exception. Surveys have shown that in 2010 in the US, 16.4% of the total energy consumed in residences was for water heating (D&R Intl. 2012). This represents 2025 PJ, or 17.7 GJ per household, at an estimated cost of $33.8 billion (US DOE 2013). During the same year in Canada, water heating was responsible for 19.5% of the total energy consumed in the residential sector. This represents 280 PJ, or 20.9 GJ per household (NRCan 2012).

Falling film Drain Water Heat Recovery (DWHR) systems could be used to reduce water heating demand. These DWHR systems are single pass, double walled, counter flow, vented heat exchangers similar to what is shown in Figures 1 and 2. They are comprised of a large diameter copper drain pipe, typically between 5.1 and 10.2 cm, which matches the size of the drain stack that they replace. Wrapped tightly around the drain pipe is a coil of smaller diameter copper tubes through which the mains water is circulated. Warm water flows into the top of the drain pipe, and exits at the base after transferring thermal energy to the cold mains-side water that enters at the bottom of the heat exchanger. Good system performance relies on a falling film of water. That is, the drain water falls as an annular film that wets the inner surface of the drain pipe. This results in high heat transfer rates by maximizing the surface area and minimizing the thickness of water through which heat must be transferred to the walls.

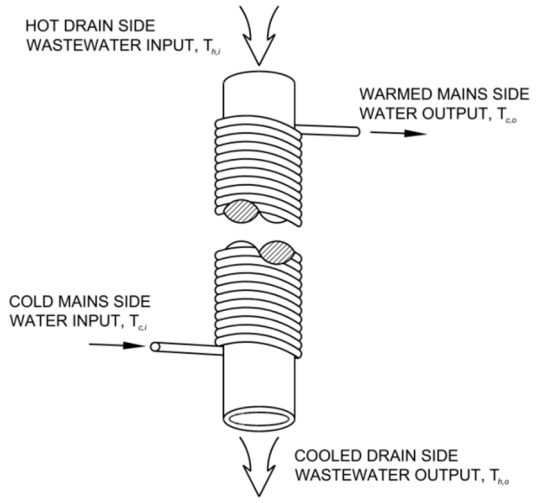

Figure 1: Schematic of a typical DWHR system (Beentjes et al. 2014).

Figure 2: Photo of common DWHR systems.

DWHR systems are becoming more common in new and energy efficient construction. In response to this, code and incentive programs are working to develop rating procedures. The Canadian Standards Association (CSA), for example, has recently produced Standard B55.1-12 *Test method for measuring efficiency and pressure loss of drain water heat recovery units* (CSA 2012). This standard includes the requirements for the design and configuration of a testing apparatus which simulates the performance of a DWHR system in a typical installation. In addition to this, the *National Energy Code of Canada for Buildings 2011* was updated in 2012 to incorporate DWHR systems (MoMA 2013), and the Government of Manitoba has mandated installation of DWHR systems in new residential buildings as of April 2016 (GoM 2015).

There is significant potential to reduce water heating demand through the use of a DWHR system. A study conducted at the Manitoba Advanced House in Winnipeg, Canada, estimated that 50% of a typical family's annual domestic hot water load could be recovered (Proskiw 1998), and subsequent Oak Ridge National Labs research produced similar results (Tomlinson 2001). Later work conducted by the Canadian Centre for Housing Technology examined DWHR systems and concluded that gas consumption for water heating could be reduced by 9 to 27% depending on system configuration (Zaloum et al. 2007). Other recent studies conducted in Canada and the Netherlands support these results (Eslami-Nejad and Bernier 2009, Schuitema et al. 2005).

Each of the previously mentioned studies focused only on proving the feasibility of using DWHR systems to reduce energy consumption. None attempted to provide an understanding of DWHR system operation, or to produce performance models of DWHR systems. Significant efforts have been made to address this issue at the University of Waterloo. One study aimed to develop the characteristic effectiveness vs. flow rate curves for multiple DWHR systems (Collins et al. 2013), while others looked at the impacts of drain-side wetting (Beentjes et al. 2014) and off-vertical system installation (Manouchehri et al. 2015). Most recently, the work of Manouchehri (2015) examined the performance of DWHR systems with respect to fluid temperatures and unequal flow rates, with the ultimate goal of predicting steady-state DWHR system performance using data obtained from the rating process. The work presented here details the results of that latest study.

METHOD

DWHR systems are rated using the ε *-NTU* method (CSA 2012, Kays and London 1984). By this method, the effectiveness, ε, is defined as the ratio of heat transfer, q, to the maximum heat transfer, q_{max}, which can occur in the heat exchanger. This effectiveness is expressed as:

$$\varepsilon = \frac{q}{q_{max}} = \frac{C_c\left(T_{c,o} - T_{c,i}\right)}{C_{min}\left(T_{h,i} - T_{c,i}\right)} = \frac{\left(\dot{m}C_p\right)_c\left(T_{c,o} - T_{c,i}\right)}{\left(\dot{m}C_p\right)_{min}\left(T_{h,i} - T_{c,i}\right)} \quad (1)$$

In the above equation, C represents the heat capacity rate (kW/°C), $\dot{m}$ is the mass flow rate (kg/s), C_p is the specific heat (kJ/kg°C), and T is the temperature (°C). The subscripts c and h refer to the cold mains-side and warm drain-side, while i and o refer to the inlet and outlet. Lastly, the subscript *min* refers to the lesser of C_c and C_h.

When the mass flow rates on both sides of the DWHR system are the same, the system is operating under equal flow conditions. By assuming that C_p is the same on both sides of the DWHR system:

$$\left(\dot{m}C_p\right)_h = \left(\dot{m}C_p\right)_c \quad (2)$$

Hence, Eqn. (1) can be simplified, and a DWHR system's equal flow effectiveness can be determined using:

$$\varepsilon = \frac{\left(T_{c,o} - T_{c,i}\right)}{\left(T_{h,i} - T_{c,i}\right)} = \frac{\left(T_{h,i} - T_{h,o}\right)}{\left(T_{h,i} - T_{c,i}\right)} \quad (3)$$

The above equation shows that the system effectiveness is simply a ratio of the inlet and outlet water temperatures. Since the purpose of a DWHR system is to preheat the cold mains-side water, the effectiveness is always calculated based on the mains-side temperatures:

$$\varepsilon = \frac{\left(T_{c,o} - T_{c,i}\right)}{\left(T_{h,i} - T_{c,i}\right)} \quad (4)$$

Equation (4) is mandated for rating DWHR systems according to CSA standard B55.1-12 (CSA 2012). It dictates that the system effectiveness be evaluated for a mains-side temperature of 12±5°C, and a drain-side at 28±1°C above the mains-side temperature, and at 6 flowrates: 5.5, 7, 9, 10, 12, 14±0.2 L/min. A curve fit of the form shown in Eqn. (5) is then fit to the data, and used to produce a single rated value at 9.5 L/min.

$$\varepsilon = \frac{1}{a\dot{V} + b} \quad (5)$$

Here, a and b are fit coefficients. $\dot{V}$ is the volumetric flow rate in L/min.

An apparatus for testing the performance of DWHR systems was built at the University of Waterloo. It is capable of providing water at prescribed mains-side and drain-side temperatures, and at a continuous flow rate for approximately 15 minutes. Inlet and outlet water temperatures are measured to within ±0.1°C. Tests can be performed for volumetric flow rates of up to 26 L/min with an accuracy of ±1% of the reading. The system is set up to permit testing both under equal flow, and non-equal flow conditions. A detailed description of this apparatus is available in a recent publication by Manouchehri (2015). It is noted that the majority of CSA testing performed in Canada has been done on this apparatus.

MODEL DEVELOPMENT

Based on the authors' experiencing in testing DWHR systems, a strategy was laid for using data obtained from the rating process, to estimate steady-state performance under real operating conditions. In brief, one must first estimate the equal flow effectiveness for the system, correct it for the inlet fluid temperatures, and if needed, use this to predict the non-equal flow performance. While each of those steps will be described in this paper, full details of the experiments and model validations can be found in the work of Manouchehri (2015).

Estimating the Rated Equal Flow Effectiveness Curve

To estimate the equal flow effectiveness curve, some data related to the DWHR system performance is needed. Three likely data sources are presented:

(1) The user may have access to CSA test data from a system manufacturer, or from CSA reports. If available, this would contain the equal flow effectiveness curve-fit in the form of Eqn. (5).

(2) The user may have equal flow effectiveness measurements taken at the CSA test flow rates of 5.5, 7, 9, 10, 12 and 14 L/min, or similar data produced from other sources. The equal flow effectiveness curve can be developed by fitting Eqn. (5) to this data. Care must be taken when doing this. At low flow rates, drain-side film stability, and therefore steady-state performance, varies between DWHR systems. When generating the curve fit, therefore, the user is advised not to use any data obtained at flowrates below 5.5 L/min, or below 7 L/min for a 10.2 cm diameter system.

(3) The final process is not advised, and should only be used for rough calculations in the absence of more data. At worst, the user will have access to the CSA label placed on the system. This will be a single equal flow effectiveness value for a flow rate of 9.5 L/min. If it is assumed that the DWHR system effectiveness approaches 80% as the flow rate goes to zero (i.e. a b coefficient of 1.25), then one could approximate the equal flow effectiveness curve by fitting Eqn. (5) through a single point.

As was mentioned previously, Option (2) is the process specified by CSA (2012) to generate the equal flow effectiveness curve mentioned in Option (1). Figure 3 shows an example of the curve fit for the 7.6 cm diameter, 122cm long system.

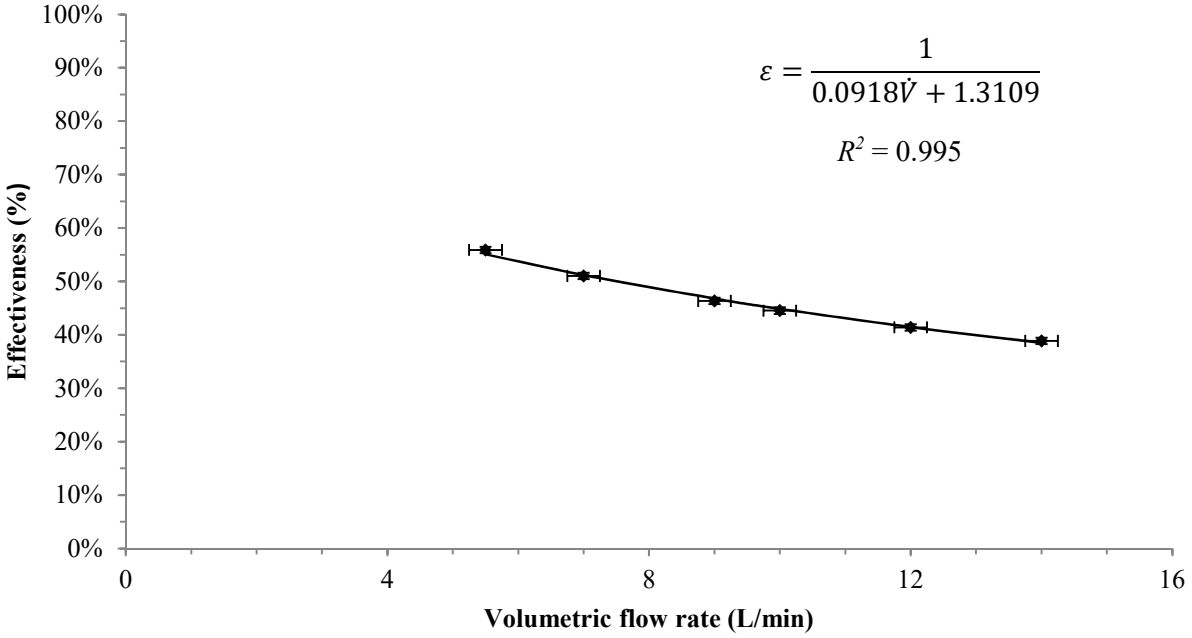

Figure 3: Equal flow effectiveness vs volumetric flow rate for a 7.6 cm diameter, 122 cm long DWHR system.

Temperature Adjustment of the Equal-Flow Effectiveness Curve

During previous experimentation, it was recognized that the inlet temperatures had an impact on the calculated effectiveness. Within the bounds of the CSA standard, if one were to test the effectiveness of a DWHR system at a mains-side of 7°C and drain-side of 35°C, and then again at 17°C and 45°C, the calculated effectiveness would increase by as much as 2%. A theoretical analysis of heat transfer in the DWHR system was conducted and successfully used to predict the impact of inlet temperatures on system effectiveness. Additionally, this work showed that much of the change in effectiveness came from changes in dynamic viscosity with temperature, and the resulting impact of this on heat transfer coefficients. It is evident that the inlet temperatures used during the production of the equal flow effectiveness curve are important, as is a correction of the curve to suit the conditions being studied by the user.

Knowledge of the inlet temperatures used to produce the equal-flow effectiveness curve is likely not an issue. For CSA rated data, it was recognized that the standard provided too much flexibly, and efforts were made to be consistent with test temperatures. As such, the vast majority of CSA testing that has taken place has been done at inlet temperatures near-to 10°C and 38°C on the mains-side and the drain-side, respectively. In any case, the actual temperatures measured during testing are required as part of the CSA test report, and those should be available to the user. For user-produced data, the temperatures will be known. If unavailable, it is suggested that the temperature correction be omitted, and an additional 2% uncertainty be added to final results.

While a temperature correction could be developed based on the aforementioned theoretical analysis, it was deemed to be overly complex. Instead, it was decided that a simpler correlation could be developed based on experimental data. Four DWHR systems were tested: two 7.6 cm diameter systems with lengths of 122 and 153 cm, and two 10.2 cm diameter systems with lengths of 122 and 153 cm. Tests were performed under equal flow conditions at flow rates of 5.5, 9.5 and 14 L/min, and inlet temperatures were chosen to be 25, 30, 35, 40 and 45°C on the drain-side, and 5, 10, 15 and 20°C on the mains-side. A minimum temperature difference of 10°C was held across the heat exchanger to maintain experimental accuracy. A sample of the results is shown in Figure 4 for the 7.6 cm diameter, 122 cm long system, and at 9.5 L/min. Results for the other systems are available from Manouchehri (2015). Error bars were determined using Moffat's (1982) method of engineering uncertainty.

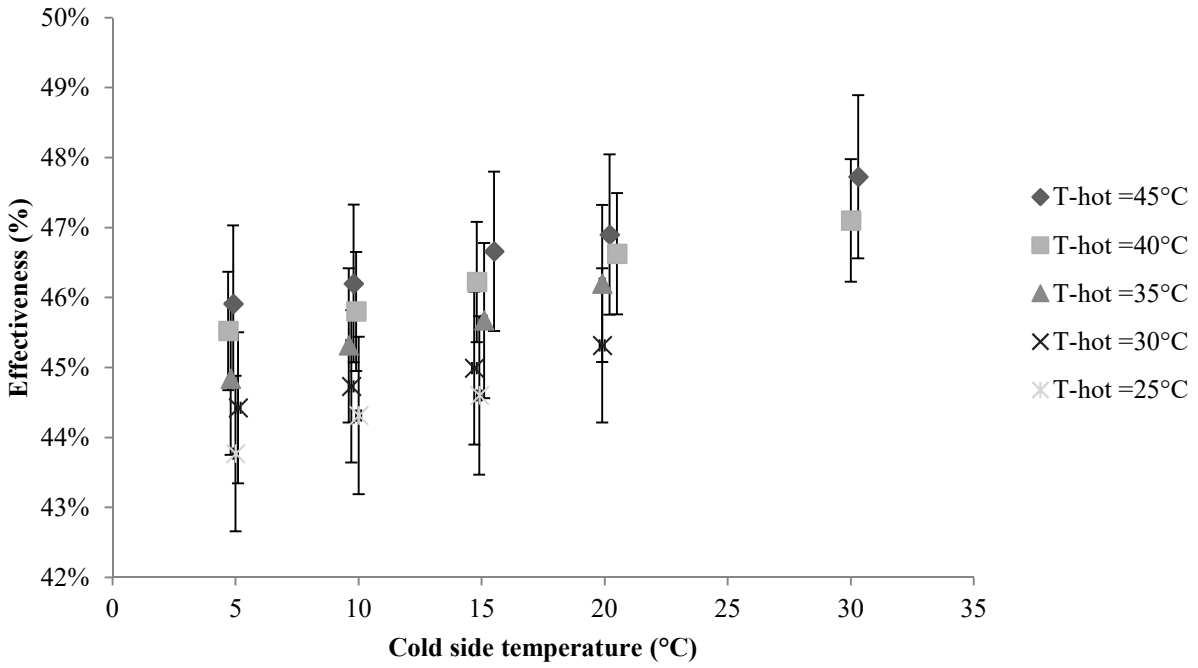

Figure 4: Measured effectiveness values for the 7.6 cm diameter, 122 cm long system, at 9.5 L/min.

In all cases, the measured system effectiveness changed with inlet temperature in a predictable way. At a constant drain-side temperature, the effectiveness increased linearly with increasing mains-side temperature. The same effect was seen when drain-side temperature was increased linearly at a constant mains-side temperature. It was decided, therefore, to develop a linear correction factor with interaction. The correction factor was to take the form

$$F_C = \frac{\varepsilon}{\varepsilon_{ref}} = A \cdot T_{h,i} \cdot T_{c,i} + B \cdot T_{h,i} + C \cdot T_{c,i} + D \quad (6)$$

where ε is the equal-flow effectiveness at a set of known inlet temperatures, ε_{ref} is the effectiveness determined at a set of inlet reference temperatures, and F_C is the correction factor. A, B, C, and D are fit coefficients. The reference temperatures were chosen to be at $T_{h,i}$ = 40°C and $T_{c,i}$ = 10°C, which are closest to the typical temperatures of the CSA test standard and the Europian standards (CSA 2012, NEN 2009). Further examination of the data showed that when applied to each data set, nearly identical correlations were produced. Therefore, a final universal temperature correction was produced using all of the data.

$$F_C = \frac{\varepsilon}{\varepsilon_{ref}} = 2.37\times10^{-6} \cdot T_{h,i} \cdot T_{c,i} + 1.75\times10^{-3} \cdot T_{h,i} + 1.24\times10^{-3} \cdot T_{c,i} + 0.917 \quad (7)$$

where all T's are input in °C. It is noted that fit coefficients used in Eqn. (7) are specific to the reference temperatures specified previously.

Equation (7) has been tested and shown to accurately correct equal flow effectiveness measurements to within ±0.2 of the measured effectiveness. Details of these tests can be found in Manouchehri (2015).

Performance at Non-Equal Flow Conditions

The final step in determining system performance is to examine conditions of non-equal flow. To do this, 5 DWHR systems were tested: one 5.1 cm diameter system with a length of 122 cm, two 7.6 cm diameter systems with lengths of 122 and 153 cm, one 10.2 cm diameter system with a length of 122 cm, and one 7.6 cm diameter system with a length of 102 cm that originated from a different manufacturer than the other 4 systems. Tests were performed at inlet temperatures of 38±1°C and 10±1°C on the drain-side and the mains-side, respectively, and at flow rates of 5.5, 7, 9, 10, 12 and 14 L/min. With one exception, 36 conditions were measured on each system, including 6 conditions with equal flow rates. For the 10.2 cm diameter system, a flow rate of 5.5 L/min was not considered on either side of the system. A sample of the results is shown in Figure 5 for the 7.6 cm diameter and 122 cm long system. Results for the other systems are available from Manouchehri (2015). Error bars were determined using Moffat's (1982) method of engineering uncertainty.

At this point, it was decided to move from an examination in terms of effectiveness, to an examination in terms of heat transfer rate, q. This was done for 2 reasons. The first was that this conversion would be needed anyways by the user at some point in order to calculate energy savings. The second was to simplify the development of a correlation. Examination of Figure 5 and Eqn. (1) shows that an inflection point will occur in the effectiveness curve when the flow rates for the drain-side and mains-side are equal. By switching to heat transfer rate, the inflection point is removed. The calculation of heat transfer rate was performed using Eqn. (1) with the assumption of constant fluid density (ρ = 1000 kg/m^3) and specific heat (C_p = 4.180 kJ/kg°C) for water.

Several attempts were made to reduce the data shown in Figure 5 to a correlation. Eventually, it was found that the data was best represented by:

$$q_{@\dot{V}_c,\dot{V}_h} = q_{eqfl@\dot{V}_c} \times \left[M \times ln\left(\frac{\dot{V}_h}{\dot{V}_c}\right) + N \right] \quad (8)$$

Here, $q_{eqfl@\dot{V}_c}$ refers to the equal flow heat transfer rate based on the mains-side volumetric flow, and $q_{@\dot{V}_c,\dot{V}_h}$ is the heat transfer rate for non-equal flow. N would ideally be 1 so that the equal flow heat transfer rate is obtained when the drain-side and mains-side flow rates were the same. As with the temperature model, this correlation turned out to be independent of DWHR system diameter, or coil design. The final correlation is:

$$q_{@\dot{V}_c,\dot{V}_h} = q_{eqfl@\dot{V}_c} \times \left[0.3452\times\ln\left(\frac{\dot{V}_h}{\dot{V}_c}\right) + 1 \right] \quad (9)$$

Figure 6 shows a sample of this correlation for the 7.6 cm diameter, 122cm long system. Independent tests of this model were conducted in the context of the overall model.

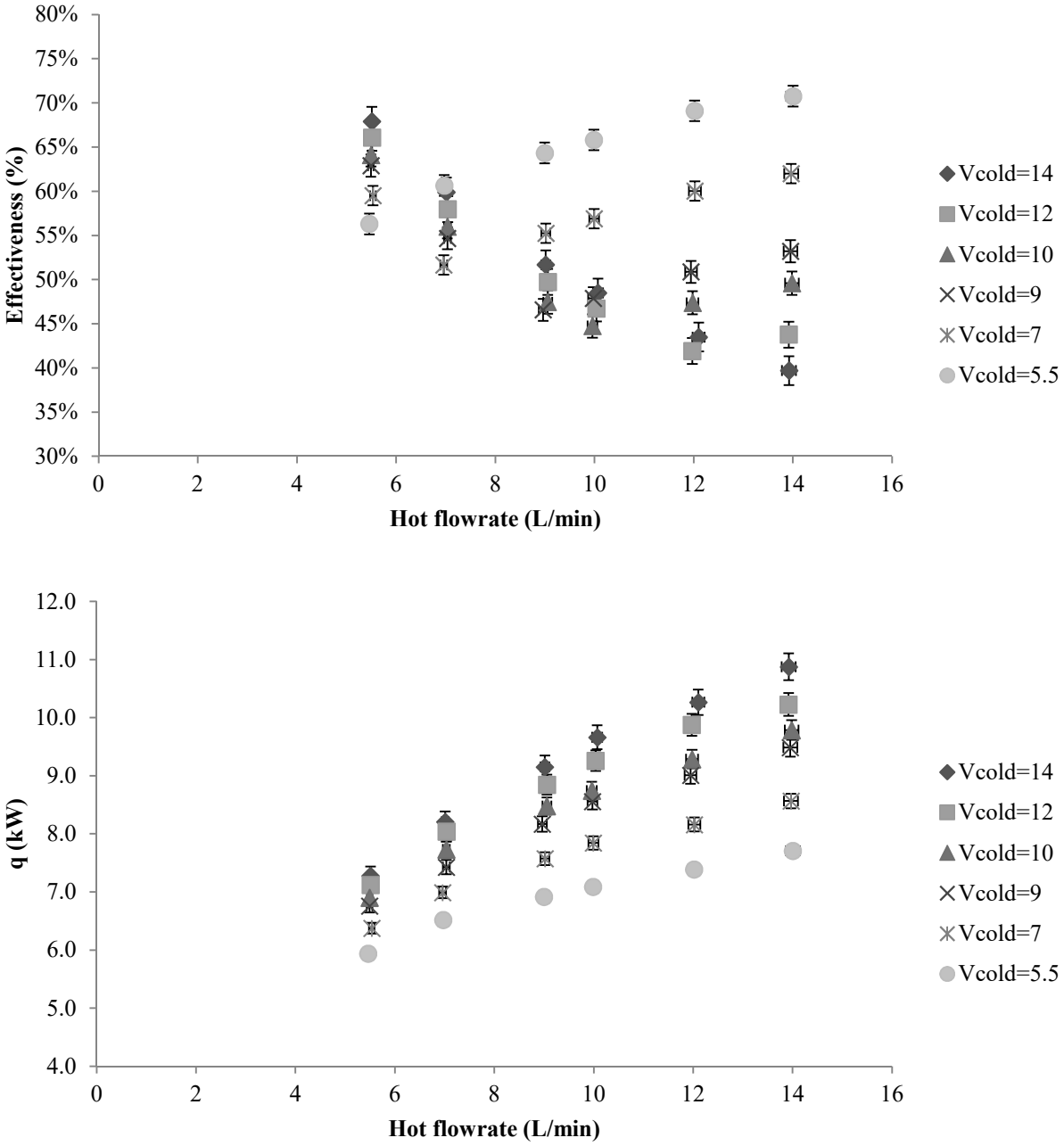

Figure 5: Mains-side effectiveness (top) and heat transfer rate (bottom) vs volumetric flow rate for the 7.6 cm diameter, 122 cm long DWHR system.

Overall Model

Using the methods presented previously, it is now possible to predict steady-state DWHR system behaviour based on equal flow data. The following process is based on a single-condition effectiveness prediction, but it can easily be expanded to examine one or more families of performance curves.

(1) Obtain the equal flow effectiveness curve. The curve may be directly available from CSA reports. If not, fit Eqn. (5) using equal flow data from CSA or an equivalent rating process. The user is advised not to use any data obtained at flowrates below 5.5 L/min, or below 7 L/min in the case of a 10.2 cm diameter system. Use this curve fit to calculate the equal flow effectiveness at the desired mains-side flow rate.

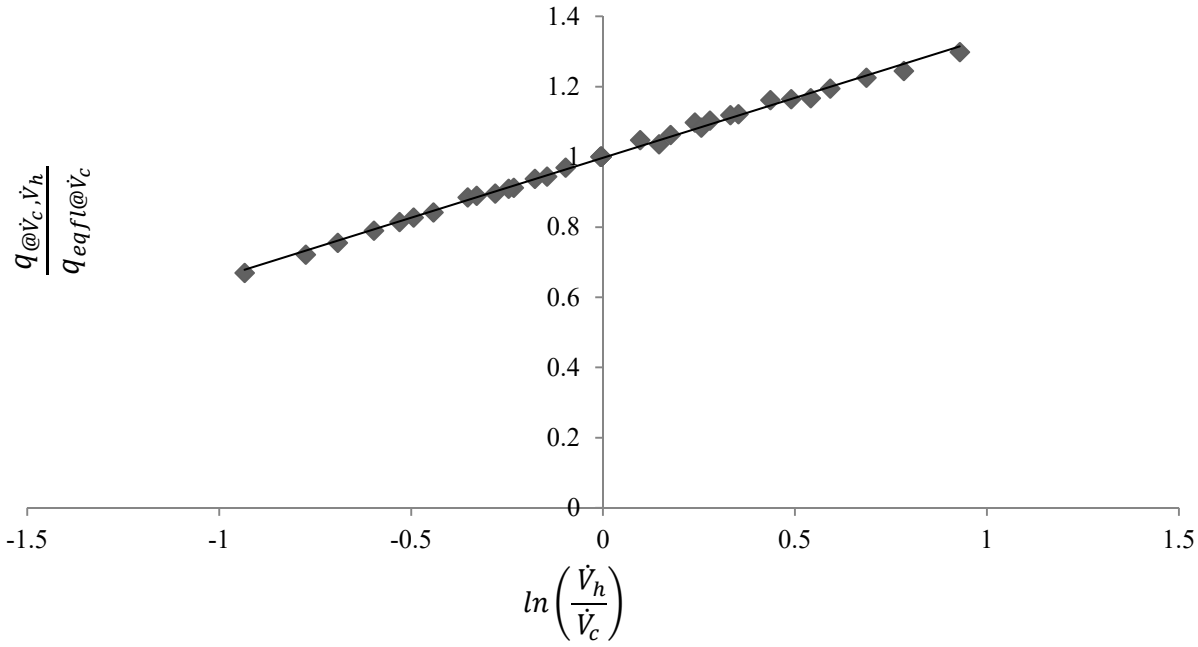

Figure 6: Normalized heat transfer data for the 7.6 cm diameter, 122 cm long DWHR system.

(2) Adjust the calculated effectiveness to represent the input temperatures being considered using Eqn. (7). This is a 2-stage process. If the effectiveness curves determined in step (1) are not taken from the reference condition of $T_{h,i}$ = 40°C and $T_{c,i}$ = 10°C, then Eqn. (7) must first be used to determine ε_{ref}. Following this, Eqn. (7) is used again to calculate ε at the inlet temperatures of interest.
(3) A conversion to heat transfer rate is required. Convert using:

$$q_{eqfl@\dot{V}_c} = \frac{4180 \times \dot{V}_C \times \varepsilon \times \left(T_{h,i} - T_{c,i}\right)}{60000} \qquad (10)$$

where $\dot{V}_C$ is the mains-side flow rate in L/min. The heat transfer rate, q , is in kW, and T's are in °C.
(4) If required, find the non-equal flow heat transfer rate using Eqn. (9).

The ranges of applicability for this process are 5°C < $T_{c,i}$ < 20°C, 25°C < $T_{h,i}$ < 45°C, and flow rates between 5.5 and 14 L/min.

VALIDATION

Four DWHR systems were chosen to validate the overall model. The systems represented 3 DWHR diameters, 3 lengths, and two different manufacturers. Table 1 lists the systems examined.

Table 1: Dimensions of DWHR systems studied.

System #	Manufacturer	Diameter cm	Length cm
1	A	5.1	122
2	A	7.6	92
3	B	7.6	102
4	B	10.2	122

Each of the DWHR systems listed were first tested at flow rates of 5.5, 7, 9, 10, 12 and 14 L/min, and at inlet temperatures of 38±1°C and 10±1°C on the drain-side and the mains-side, respectively, in order to produce the CSA data. Each system was then tested at random conditions with varying temperatures and flow rates through either side of the system. Performance predictions were then compared to measured results. In total, 21 validation cases were considered.

The calculation procedure is demonstrated for one of these cases. The 7.6 cm diameter and 92 cm long DWHR system (System #2) was first tested to produce the CSA data for the system. This data is shown in Table 2 with the curve fit as Eqn. (11).

Table 2: CSA data for System #2.

$\dot{V}$ L/min	ε %	q kW
5.50	49.6	5.26
7.00	44.3	6.01
9.01	39.4	6.96
10.01	37.7	7.38
12.02	35.0	8.27
14.02	32.9	9.11

$$\varepsilon = \frac{1}{0.1188\dot{V} + 1.4207} \tag{11}$$

The random retest of System #2 was then performed. In this case, $T_{c,i}$ = 14.6°C, $T_{h,i}$ = 44.9°C, a mains-side flowrate of 13.0 L/min, and a drain-side flow rate of 10.5 L/min were used. The measured steady-state heat transfer rate for this test was 8.87 kW. Following the procedure described in the previous section, one would first obtain the equal flow effectiveness for this DWHR system, and use it to determine the equal flow effectiveness at the mains-side flow rate.

$$\begin{aligned}\varepsilon &= \frac{1}{0.1188(13.0) + 1.4207} \\ &= 0.338\end{aligned} \tag{12}$$

This effectiveness is then adjusted for temperature using Eqn. (7). First the reference effectiveness is determined at $T_{c,i}$ = 10.0°C, $T_{h,i}$ = 40.0°C.

$$\begin{aligned}F_C &= 2.37\times10^{-6}\cdot 38\cdot 10 \\ &\quad + 1.75\times10^{-3}\cdot 38 \\ &\quad + 1.24\times10^{-3}\cdot 10 \\ &\quad + 0.917 \\ &= \frac{0.338}{\varepsilon_{ref}}\end{aligned} \tag{13}$$

Solving gives a value of ε_{ref} = 0.339. The effectiveness for the temperatures experienced during the validation test is then calculated.

$$\begin{aligned}F_C &= 2.37\times10^{-6}\cdot 44.9\cdot 14.6 \\ &\quad + 1.75\times10^{-3}\cdot 44.9 \\ &\quad + 1.24\times10^{-3}\cdot 14.6 \\ &\quad + 0.917 \\ &= \frac{\varepsilon}{0.339}\end{aligned} \tag{14}$$

Solving gives a temperature corrected equal flow effectiveness value of ε = 0.344. Effectiveness is then converted to heat transfer rate using Eqn. (10).

$$q_{eqfl@\dot{V}_c} = \frac{4180\times13.0\times0.344\times(44.9-14.6)}{60000} \tag{15}$$

giving $q_{eqfl@\dot{V}_c}$ = 9.43 kW. Finally, Eqn. (9) is applied to account for non-equal flow.

$$q_{@\dot{V}_c,\dot{V}_h} = 9.43\times\left[0.3452\times\ln\left(\frac{10.5}{13.0}\right)+1\right] \tag{16}$$

giving $q_{@\dot{V}_c,\dot{V}_h}$ = 8.74 kW. This is 0.13 kW lower than the measured value with a prediction error of 1.5%. A complete listing of the validation cases along with prediction errors are shown in Table 3, and can be found in Manouchehri (2015).

CONCLUSIONS

Several DWHR systems, representing different diameters, lengths, and manufacturers, were tested as part of the work presented. Methods were developed and validated for determining the equal flow effectiveness curve, to correct for inlet temperatures, and to predict the impact of non-equal flow conditions. In each case, these corrections turned out to be universal.

The procedure was then used to predict the heat transfer rates for 21 cases. Model predictions were in good agreement with the measured values. The maximum percent error between the predicted and measured heat transfer rates among these cases was usually less than 2.5%. This is a clear indication of how effective the overall model is at predicting the steady-state heat transfer rates. The range of model applicability is 5°C < $T_{c,i}$ < 20°C, 25°C < $T_{h,i}$ < 45°C, and flow rates between 5.5 and 14 L/min. The correlations developed here only apply to falling film DWHR systems that consist of a large pipe wrapped with smaller tubes, and operating in a counter-flow arrangement.

Table 3: Measured and predicted heat transfer rates for all validation tests.

Test #	System #	$T_{c,i}$ °C	$T_{h,i}$ °C	$\dot{V}_c$ L/min	$\dot{V}_h$ L/min	ε %	Measured q kW	Predicted q kW	Percent Difference
1	1	10.7	42.6	9.97	6.04	54.0	7.25	7.32	0.92%
2	1	3.5	28.2	7.47	13.01	50.2	6.45	6.59	2.20%
3	1	3.5	27.9	5.49	11.48	59.2	5.53	5.56	0.49%
4	2	14.6	44.9	12.98	10.53	39.9	8.87	8.74	-1.51%
5	2	14.7	44.6	7.96	6.03	51.5	6.47	6.45	-0.31%
6	2	4.8	35.1	7.99	13.50	47.5	8.01	8.30	3.53%
7	2	4.8	34.9	6.02	10.97	54.5	6.88	7.05	2.40%
8	3	14.6	44.9	14.02	13.93	36.4	10.71	10.54	-1.63%
9	3	14.7	44.7	9.00	8.96	43.4	8.16	8.21	0.65%
10	3	14.8	44.4	5.47	5.42	52.7	5.89	5.79	-1.67%
11	3	14.9	45.0	14.01	10.05	45.2	9.52	9.30	-2.34%
12	3	14.9	44.8	11.97	9.03	46.6	8.76	8.69	-0.77%
13	3	4.8	35.1	14.06	13.97	34.9	10.29	10.23	-0.61%
14	3	4.8	35.0	9.00	8.92	41.9	7.85	7.96	1.33%
15	3	5.1	34.8	5.49	5.44	51.2	5.77	5.67	-1.79%
16	3	4.8	35.1	9.03	13.99	47.3	9.02	9.30	2.96%
17	3	4.8	35.0	7.03	9.99	51.0	7.55	7.71	2.14%
18	4	12.2	37.1	12.99	9.50	54.0	8.90	8.81	-1.09%
19	4	12.2	36.9	9.98	8.07	55.7	7.73	7.66	-0.88%
20	4	7.1	34.8	10.53	13.49	50.0	10.14	10.30	1.58%
21	4	7.0	34.2	8.51	12.46	56.2	9.05	9.11	0.66%

ACKNOWLEDGEMENTS

The NSERC Solar Net-Zero Energy Buildings Research Network is acknowledged for their support of this work.

The efforts of Carsen Banister and Ivan Beentjes are also acknowledged.

REFERENCES

Beentjes, I., Manouchehri, R., and Collins, M.R. (2014) 'An Investigation of Drain-Side Wetting on the Performance of Falling-Film Drain Water Heat Recovery Systems', Energy and Buildings, Vol. 82, pp. 660-667.

Collins, M.R., Van Decker, G.W.E, Murray, J. (2013) 'Characteristic Effectiveness Curves for Falling-Film Drain Water Heat Recovery Systems', HVAC&R Research, Vol. 19(6), pp. 649-662.

CSA Standard B55-10 (2012) 'Test Method for Measuring Efficiency and Pressure Loss of Drain Water Heat Recovery Units', Canadian Standards Association.

D&R International Ltd. (2012) , 'Buildings Energy Data Book', Accessed on 04/01/2016. http://buildingsdatabook.eren.doe.gov/docs%5CDataBooks%5C2011_BEDB.pdf.

Eslami-Nejad, P., and Bernier, M. (2009) 'Impact of Grey Water Heat Recovery on the Electrical Demand of Domestic Hot Water Heaters', Eleventh International IBPSA Conference, Glasgow, pp. 681-687.

Government of Manitoba (2015) 'Manitoba Building Code Amendment; The Buildings and Mobile Homes Act', Accessed on 03/01/2015. http://web2.gov.mb.ca/laws/regs/annual/2015/052.pdf

Kays, W.M., and London, A.L. (1984) 'Compact Heat Exchangers', Compact Heat Exchangers, Stanford: McGraw-Hill Book Company, pp. 14-20.

Manouchehri, R., Banister, C.J. and Collins, M.R. (2015) 'Impact of Small Tilt Angles on the Performance of Falling-Film Drain Water Heat Recovery Systems', Energy and Buildings, Vol. 102, pp. 181-186.

Manouchehri, R. (2015) 'Predicting Steady-State Performance of Falling-Film Drain Water Heat Recovery Systems from Rating Data', MASc Thesis. https://uwspace.uwaterloo.ca/handle/10012/10035

Ministry of Municipal Affairs and Housing Building and Development Branch (2013) '2006 Building Code - Supplementary Standards', Supplementary Standard SB-12 Energy Efficiency for Housing, Queen's Printer, Ontario.

Moffat, R.J. (1982) 'Contributions to the Theory of Single-Sample Uncertainty Analysis', Transactions of the ASME, Vol. 104, pp. 250-258.

Natural Resources Canada (2012), 'Residential Sector Secondary Energy Use and GHG Emissions by End-Use', Accessed on 04/01/2016. http://oee.nrcan.gc.ca/corporate/statistics/neud/dpa/data_e/downloads/comprehensive/Excel/2012/res_ca_2_e.xls.

Netherlands Normalisatie Instituut (NEN) (2009) 5128+A1, Energieprestatie Van Woonfuncties en Woongebouwen – Bepalingsmethode.

Proskiw, G. (1998), 'Technology Profile: Residential Greywater Heat Recovery Systems', Ottawa, The CANMET Energy Technology Centre (CETC) Energy Technology Branch, Department of Natural Resources Canada

Schuitema, R., Sijpheer, N.C., and Bakker, E.J. (2005) 'Energy Performance of a Drainwater Heat Recovery System', European Conference and Cooperation Exchange on Sustainable Energy, Vienna.

Tomlinson, J.J., (2001), 'Heat Recovery from Wastewater using a Gravity-Film Heat Exchanger', Federal Energy Management Program. Oak Ridge National Laboratory

U.S. Department of Energy's Office of Energy Efficiency & Renewable Energy (2013), ' Hot Showers, Fresh Laundry, Clean Dishes ', Accessed on 04/01/2016. http://energy.gov/eere/buildings/articles/hot-showers-fresh-laundry-clean-dishes.

Zaloum, C., Gusdorf, J., and Parekh, A. (2007) 'Performance Evaluation of Drain Water Heat Recovery Technology at the Canadian Centre for Housing Technology', Sustainable Buildings and Communities, National Resources Canada, Ottawa.